

Study of Two Coupled Sites in Nd³⁺:KLiYF₅

H. Weidner, P. L. Summers, R. E. Peale, and B. H. T. Chai

University of Central Florida, Department of Physics, Orlando, Florida 32816

B. H. T. Chai is also with CREOL, University of Central Florida, Orlando, Florida 32826

ABSTRACT

High resolution spectroscopy of Nd³⁺ in Potassium Lithium Yttrium Fluoride (KLiYF₅) at ≤80 K reveals two crystal-field sites which are equally populated independent of concentration. Site selective excitation of photoluminescence distinguishes each site's contribution to the spectra. The analysis of integrated line intensities reveals a bidirectional energy transfer between Nd³⁺ ions in different sites. The energy transfer rate increases rapidly with Nd concentration and depends strongly on temperature (2 K - 80 K).

Advances in semiconductor-laser technology have revived the interest in rare-earth activated insulators suitable for diode-pumped lasing. In particular, powerful AlGaAs diode lasers are well suited to pump an absorption band at 0.8 μm for lasing at 1 μm in Nd³⁺ activated materials. Still, considerable improvements over traditional materials such as Nd:YAG are required before practical miniaturized all solid-state 1 μm lasers can be realized. In this context, we have grown and studied the new crystal KLiYF₅ (KLYF) activated by Nd³⁺ ions. As a laser medium Nd:KLYF was recently reported to have low threshold and high gain [1,2].

In the course of spectroscopic characterization of our KLYF crystals, new features were revealed that had been missed in previous low resolution studies. Our high resolution spectroscopy reveals, in contradiction to the spectroscopic results of Kaminskii and Khaidukov [1], that the Nd³⁺ ions occupy two similar sites which have measurably different crystal fields [3]. The two sites are occupied nearly equally by the dopant Nd³⁺ ions. With site selective spectroscopy, we separated the

contributions of each site to the spectra and separately determined the energy levels [3]. Here we discovered that the ability to selectively excite luminescence from a single site decreases dramatically with increasing Nd concentration. Energy transfer between sites is responsible for the decreasing selectivity. Since energy transfer can significantly alter the laser performance of any solid state laser, it is important to study and understand it in detail. KLYF with its two very similar sites is an interesting model system for this purpose. The technique we used to study the transfer is based on high resolution transmission and photoluminescence spectra obtained in a cw-regime and does not require high spectral- and time-resolution simultaneously. Steady state solutions to simple rate equations are combined with luminescence intensity ratios and independent low resolution fluorescence life time measurements to give the transfer rates. Repeating the experiments at different temperatures reveals a significant temperature dependence of the transfer process.

Table I. Nominal and actual concentrations, fluorescence life times and inverse intersite transfer rates for Nd³⁺:KLYF₅ at 80 K.

concentration (%)		fluorescence	inv. transfer
nominal	actual	life time (μs)	rate 1/C (μs)
0.2	0.2	521	2110
2.0	1.5	482	118
3.3	2.4	411	62
5.0	3.4	349	24

The crystals were grown by the top-seeded solution growth method with nominal Nd³⁺ concentrations of

0.2%, 2.0%, 3.3%, and 5.0%. The actual Nd^{3+} concentrations (see Table I) in the samples were determined with the help of Rutherford Back Scattering of He^+ (1.7 MeV) and the software program RUBSODY. The density of Nd^{3+} ions is then the corresponding fraction of the Yttrium concentration, which is $9.14 \times 10^{21} \text{ cm}^{-3}$ for undoped crystals [4]. The large optical quality, light violet, monoclinic [4] crystals were oriented for polarized measurements by means of cleavage planes which define the crystallographic b axis.

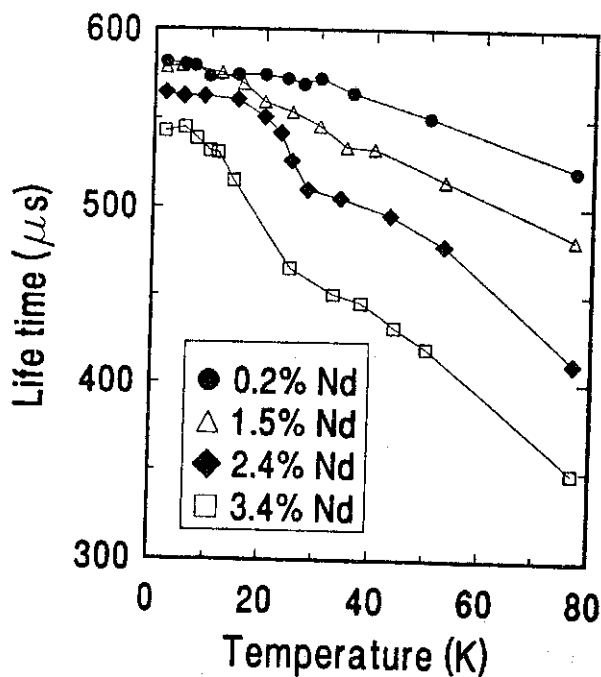


Figure 1. Fluorescence life times of the ${}^4\text{F}_{3/2}$ level for different Nd concentrations as functions of temperature.

Both photoluminescence and absorption spectra were taken with a Bomem DA8 Fourier transform spectrometer. The detector was a silicon photodiode, the beamsplitter quartz, and the source for transmittance a quartz-halogen lamp. An InSb detector allowed the simultaneous measurement of all ${}^4\text{F}_{3/2}$ emission. Its response was corrected using the known emission spectrum of a quartz-halogen lamp. A jet-dye laser (dyes: DCM and LDS821) pumped by a multi-line Argon-ion laser was used for site selective excitation of photoluminescence. The laser frequency was selected with a birefringent plate ($\Delta\nu = \pm 3 \text{ cm}^{-1}$) calibrated by directly measuring the laser output with the Fourier spectrometer. The FWHM of the laser output was $\leq 2 \text{ cm}^{-1}$. The width of the beam was slightly larger than the sample ($\sim 10 \text{ mm}$) which allowed, together with weak absorption, for a uniform excitation within the sample volume. Measurements at 80 K made use of a home-

made liquid-nitrogen cold-finger cryostat. Measurements below 80 K were performed with a Janis supervaritemp liquid-helium cryostat.

For fluorescence lifetime measurements, the samples were excited with filtered light (13000 to 18200 cm^{-1}) from a flash lamp giving pulses of $30 \mu\text{s}$ duration with a repetition rate of about 2 Hz. The sample emission passed a low-pass filter ($\leq 12800 \text{ cm}^{-1}$), was detected with a silicon detector, and was digitally recorded as a function of time with a time resolution of $5.6 \mu\text{s}$. The decays are adequately described by a single exponential function, which indicates that the decay rates of both sites are approximately equal. Since the emission from the ${}^4\text{F}_{3/2}$ levels dominates in the detected range, the obtained $1/e$ decay times represent the lifetimes of the ${}^4\text{F}_{3/2}$ manifold of Nd^{3+} in the different samples. The temperature dependence of the fluorescence life times is shown in Fig. 1. The life times behave essentially as expected: higher concentrations have shorter life times which decrease with raising temperature. There appears to be an additional reduction of life time at about 30 K (at least at high Nd concentrations) which is however small ($< 10\%$). The decay times at 80 K are also given in Table I.

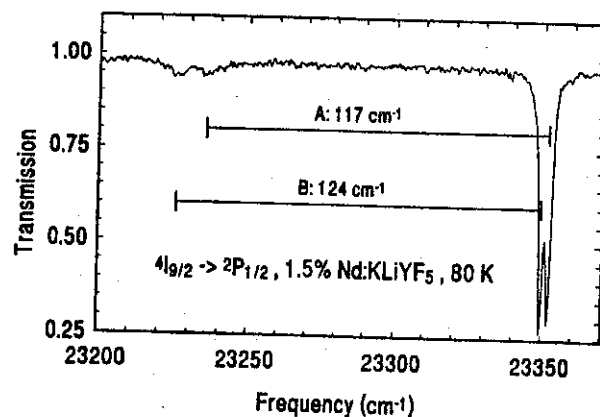


Figure 2. The ${}^2\text{P}_{1/2}$ transmission spectrum at 80 K shows the absorption of Nd^{3+} in two sites.

Evidence for the existence of two distinct crystal-field environments for Nd dopant ions is presented in Fig. 2. It shows the unpolarized transmission spectrum containing the transitions from the ground level and from the thermally populated first excited level to the ${}^2\text{P}_{1/2}$ level. In both cases, there are clearly two lines - one for each site. The differences of the center frequencies as indicated in Fig. 2 agree with the energies of the first excited levels of 115.6 cm^{-1} and 123.5 cm^{-1} for site A and B, respectively [3]. (The weakness of the thermal replica causes an uncertainty of $\pm 2 \text{ cm}^{-1}$.) Thus, this spectrum is clear evidence for the existence of two about equally populated sites in

Nd:KLYF. This complements earlier results [3] obtained with site selective excitation of photoluminescence.

Energy transfer between the two sites was observed by tuning the pump laser through a pair of absorption lines (one line of each site) and measuring the photoluminescence originating in each site. Due to the similarity of the sites, this requires high resolution spectra ($\leq 1 \text{ cm}^{-1}$) to separate each site's contribution. Ratios of integrated line strengths were determined to quantify the energy-transfer effect. These ratios were taken between members of emission-line pairs with one line from each site, i.e. I_A/I_B . The integrated line intensities I_A and I_B were obtained from nonlinear least squares fits of Voigtian lines to the photoluminescence spectra. In these ratios, uncertainties in the total intensity due to fluctuations in laser power or alignment are divided out. This method of analysis has been widely used in energy transfer studies [5,6]. A comparison of intensity ratios vs. excitation frequency for the four different concentrations at 80 K is shown

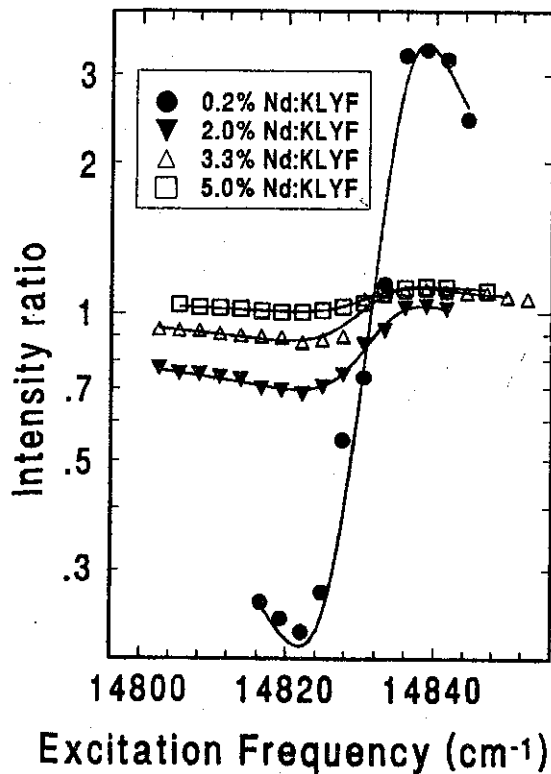


Figure 3. Intensity ratios I_A/I_B of the 9536 cm^{-1} and 9545 cm^{-1} PL lines vs. excitation frequency. (symbols = experiment; curves = fits according to our model).

in Fig. 3. The symbols represent the ratios obtained from the spectra whereas the lines are theoretical fits using the model presented below. The 3 cm^{-1}

uncertainty in excitation frequency is sufficient to explain the discrepancies between points and curves. The maximum error of the intensity ratios was estimated to be 5%. All curves have their minimum value near the maximum absorption of site B and a maximum near the absorption peak of site A [3]. The difference between maxima and minima decreases with increasing concentration. Evidently, energy transfer increases with concentration and tends to equilibrate the emission from both sites regardless of which site is resonantly excited by the laser. Another feature of the intensity ratios is remarkable: The maxima and minima lie symmetrically about a ratio not quite equal to unity. The point of symmetry varies for different (A,B) transition pairs. All curves for a given Nd^{3+} concentration are parallel but shifted, which means that ratios for different (A,B) pairs differ by a constant factor. Both the concentration dependence of the maxima-minima difference and the shift will be explained by our model.

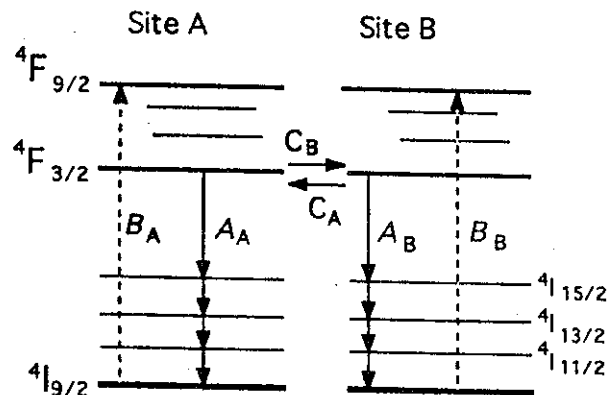


Figure 4. Schematic level diagram for Nd^{3+} in each site and important transition rates. A_i = spontaneous decay; B_i = absorption; C_i = transfer into site i .

Fig. 4 shows schematically the energy-level diagrams for the two sites and the important transition. B_A and B_B are the Einstein coefficients for the absorption process in site A and B, respectively. From the ${}^4F_{9/2}$ manifold [7], the ions relax rapidly and non-radiatively to the ${}^4F_{3/2}$ manifold. A_A and A_B are the Einstein coefficients for the total decay rates of the ${}^4F_{3/2}$ levels. The C_B and C_A are concentration dependent transfer rates towards site B and A, respectively. Using these coefficients one obtains the following rate equations [5,6,8]:

$$dn_A/dt = -A_A n_A + B_A u N_A - C_B n_A + C_A n_B \quad (1)$$

$$dn_B/dt = -A_B n_B + B_B u N_B - C_A n_B + C_B n_A \quad (2)$$

where the N_i are the numbers of Nd^{3+} ions per unit volume in site i , and n_i the number of these per unit volume in excited ${}^4F_{3/2}$ states. The energy density of the pump light is u . The assumption $n_i \ll N_i$ was made (no stimulated emission, no depletion of the ground state). This is reasonable for the pump power used of <100 mW distributed over a sample volume of >0.1 cm³. In such a low-power regime, each excitation can be treated as spatially and temporally isolated and behaves according to the probabilities for its decay, diffusion, and transfer. Therefore, the n_i are proportional to the pump intensity, and hence the intensity ratios of the emission and the transfer rates are independent of pump power.

Assuming that the laser line is much more narrow than the absorption line, $B_i u$ can be replaced by α_i/N_i times the photon flux density of the pump source. Here α_i is the site i absorption coefficient obtained from transmission spectra. Further simplifications follow from the similarities of the two sites ($A_A = A_B = A$, $C_A = C_B = C$). Steady state solutions ($dn_i/dt = 0$) give the n_i and the emission intensities $I_{ij} = b_{ij} n_i$. Index i distinguishes the two sites and index j numbers individual transitions. The proportionality factor b_{ij} includes the oscillator strength of the j^{th} transition at site i , the energy of the emitted photon and the experimental response function. Only the n_i are effected by tuning the excitation. Connection to the experiment is made by taking the ratio:

$$I_{Aj}/I_{Bj} = (b_{Aj}/b_{Bj}) \cdot \frac{(\alpha_A + \alpha_B) \cdot C/A + \alpha_A}{(\alpha_A + \alpha_B) \cdot C/A + \alpha_B} \quad (3)$$

Adjusting the two free parameters in Eq. 3 (b_{Aj}/b_{Bj} and C/A) to fit the experimental intensity ratios leads to the curves in Fig. 3. The vertical shifting observed for the actual data is achieved by varying b_{Aj}/b_{Bj} , indicating that relative oscillator strengths for the two sites differ from transition to transition. Since b_{Aj}/b_{Bj} is always close to unity, the difference is slight. This is confirmed in absorption spectra because lines belonging to a pair are always about equally strong (see Fig. 2 and Ref. [3]). Varying C/A in Eq. 3 changes the difference between maximum and minimum: Increasing C/A makes the intensity ratio more nearly equal to b_{Aj}/b_{Bj} and independent of excitation frequency. The observed decrease in the variation of the intensity ratio with increasing concentration (Fig. 3) is therefore explained by an increase in C/A . With A (the inverse of the fluorescence life time) and the fits of Eq. 3 to our data, we obtain the transfer rate C for each concentration. The 80 K transfer times ($1/C$) for our samples are

given in Table I.

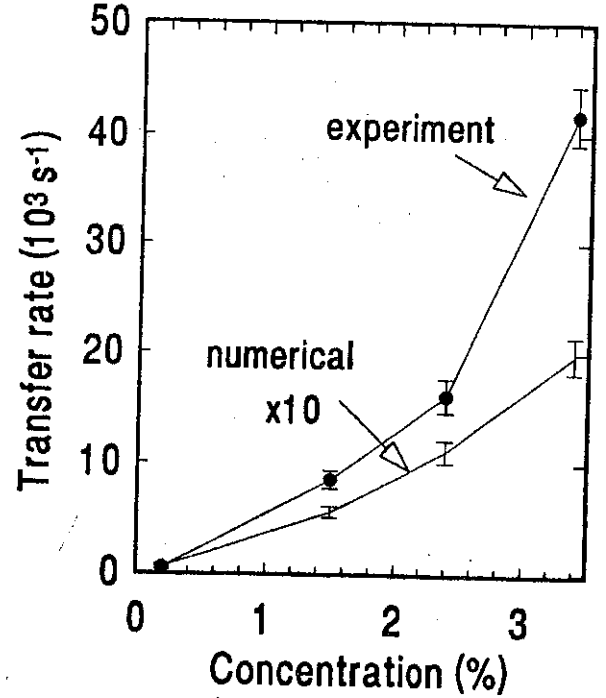


Figure 5. Concentration dependence of the transfer rate C at 80 K. The numerical simulation does not match in magnitude and concentration dependence.

Fig. 5 presents the concentration dependence of C at a temperature of 80 K. It shows a more than quadratic increase of the transfer rate with increasing concentration. Also shown are the results of numerical simulations. Using Dexter's [9] result for a dipole-dipole interaction involving the overlap of ${}^4F_{3/2}$ emission and the absorption to this manifold, one can calculate the transfer probability rate between two ions (refractive index at 632.8 nm: 1.44). The simulation distributes approximately 600 Nd^{3+} ions in a KLYF lattice, determines for each ion the transfer rates to the 16 closest partners, places randomly one excitation at a time, tracks its behavior, and counts the decays (assumed to be radiative) for each site. Eq. 3 can then be used to find the transfer rates plotted in Fig. 4 (magnified by a factor of 10). The numerical simulation automatically includes energy transfer, back transfer, and migration of energy among ions of the same site type. There are no restrictions regarding the relative strength of these processes. (This has not yet been achieved by analytical methods.) It does not include any free parameter besides the assumption of a random ion distribution. Fig. 5 shows that the dipole-dipole model severely underestimates the magnitude of the transfer rate and also does not reproduce the concentration dependence of the experimental results. It

is unclear at this time how to explain the observed large transfer rates. Interestingly, the transfer rates are even higher at about 30 K. Fig. 6 shows the temperature

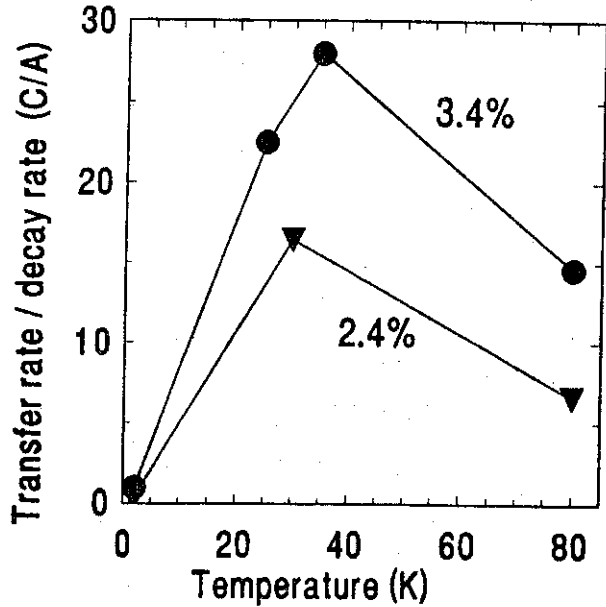


Figure 6. Temperature dependence of the ratio of transfer and decay rate (C/A) for the two highest concentration samples.

dependence of the fitting parameter C/A for the two highest concentrations. After a rapid increase below 30 K, C/A drops at 80 K to less than half of the maximum value. As mentioned earlier, the changes in the life time are small and can not be responsible for the peak in C/A . Additional temperature dependent measurements are being performed to clarify this unusual effect.

To summarize, we have shown that Nd^{3+} dopant ions in the two different crystal-field sites of KLYF exchange energy via bidirectional transfer. The transfer rate increases rapidly with increasing Nd^{3+} concentration and varies strongly in the range from 2 K to 80 K. We view Nd:KLYF as a model system for studying energy transfer in multisite crystals. The use of high resolution Fourier spectroscopy, cw site-selective excitation, and a concentration series to study energy transfer is in principle applicable also to a wide range of other materials.

- B. H. T. Chai, *J. Appl. Phys.* **75**, issue 4 (1994)
4. A. V. Goryunov, A. I. Popov, and N. M. Khajdukov, *Mat. Res. Bull.* **27**, 213 (1992).
5. L. D. Merkle and R. C. Powell, *Phys. Rev. B* **20**, 75 (1979).
6. M. Zokai, R. C. Powell, G. F. Imbusch, and B. Di Bartolo, *J. Appl. Phys.* **50**, 5930 (1979).
7. The results were checked using a LDS821 dye. The excitation was then into the upper $^4F_{3/2}$ level.
8. J. K. Tyminski, C. M. Lawson, and R. C. Powell, *J. Chem. Phys.* **77**, 4318 (1982).
9. D. L. Dexter, *J. Chem. Phys.* **21**, 836 (1953).

1. A. A. Kaminskii and N. M. Khaidukov, *Phys. Stat. Sol. (a)* **129**, K65 (1992).
2. J. F. H. Nicholls, X. X. Zhang, G. D. Loutts, B. Henderson, M. Bass, and B. H. T. Chai, in *Growth, Characterization, and Applications of Laser Host and Non-linear Crystals II*, B. H. T. Chai, ed. *proc. SPIE* 1863, (1993), Vol. 13.
3. P. L. Summers, H. Weidner, R. E. Peale, and